PERGAMON

Deep-Sea Research II 49 (2002) 4131–4144

DEEP-SEA RESEARCH
PART II

www.elsevier.com/locate/dsr2

Exchange of planktonic biomass through the Strait of Gibraltar in late summer conditions

A. Reul[a,*], J.M. Vargas[b], F. Jiménez-Gómez[c], F. Echevarría[d], J. García-Lafuente[b], J. Rodríguez[a]

[a] *Departamento de Ecología, Universidad de Málaga, Campus de Teatinos, 29071 Málaga, Spain*
[b] *Departamento de Física Aplicada II, Universidad de Málaga,Campus de Teatinos, 29071 Málaga, Spain*
[c] *Departamento de Biología Animal, Vegetal y Ecología Universidad de Jaén, Las Lagunillas, 23071 Jaén, Spain*
[d] *Departamento de Ecología, Facultad de Ciencias del Mar, Universidad de Cádiz, 11510 Puerto Real, Cádiz, Spain*

Received 13 April 2000; received in revised form 30 March 2001; accepted 19 April 2001

Abstract

In order to estimate plankton biomass transport through the Gibraltar Strait, plankton biomass and velocity profiles were measured at three stations located in the eastern side of the Strait as a part of the CANIGO project. Abundance and biomass measurements were carried out for autotrophic (*Prochlorococcus*, *Synechococcus* and eukaryotic pico-nano- and microplankton) and heterotrophic (bacteria and nanoflagellates) organisms, in September 1997. Biomass and velocity decreased from the surface to deeper water. Highest biomass concentration was observed at the northern station (0.12 g C m^{-3}), whereas maximum mean velocities (80 cm s^{-1}) were found at the central and southern stations. Biomass transport is estimated with a approach with a 10 -m resolution in the vertical and three subareas of approximately 5 km in the horizontal direction. Estimate of plankton biomass transports towards the Mediterranean and the Atlantic are 5570 and 1140 tonnes C day^{-1}, respectively. The former is co-dominated by heterotrophic bacteria (37%) and autotrophic nanoplankton (42%), while the latter is dominated by heterotrophic organisms like bacteria (75%) and heterotrophic nanoflagellates (14%). The variation during a one-day period of the biomass transport estimate at the central part of the Strait was explored. Also, in order to estimate the influence of spatial distribution of both biomass and velocity in the transport estimates, a comparison of our results with other possible estimates performed with less spatial resolution is carried out. The results confirms that both temporal and spatial resolution are key factors for transport estimates of inhomogeneous distributed variables through the Strait.

1. Introduction

Historically, the mean water exchange through the Strait of Gibraltar has been recognised as a density-driven, two-layer flow that compensates for the loss of buoyancy of the Mediterranean Sea. The inflowing and outflowing fluxes involved are of the order of 1 Sv (1 Sv = 10^6 m^3 s^{-1}). The underlying physical mechanisms that govern this exchange are well understood, although some questions (i.e. the exact value of the exchanged transports) are still debated (Lacombe and Richez, 1982; Gascard and Richez, 1985; Armi and Farmer, 1985, 1988; Bryden and Kinder, 1991;

*Corresponding author. Tel.: +34-952-13-2386; fax: +34-952-13-2000.
E-mail address: areul@uma.es (A. Reul).

0967-0645/02/$ - see front matter
PII: S0967-0645(02)00146-7

Bryden et al., 1994, for a complete summary). Biogeochemical balances are much more scarce even though there is fundamental ecological question related with the trophic state of the Mediterranean ecosystem. Coste et al. (1988) described a nutrient deficit for the Mediterranean linked to the water exchange through the Gibraltar Strait, which appeared to be compensated by the input from river runoff. Furthermore, the Mediterranean was suggested to be an active area for mineralization, indicated by the differences in dissolved organic nitrogen and particulate organic nitrogen concentrations between inflow and outflow. If so, the Mediterranean should have a net biomass import, and a higher relation of autotrophic to heterotrophic organisms in the inflowing than in the outflowing water. The amount of living biomass (carbon) is not comparable with that within the pool of particulate (non-living) or dissolved organic matter. However, its fast turnover rate makes it crucial for the dynamics of the pelagic ecosystem at both sides of the Strait. Nevertheless, there was no estimate of living plankton biomass exchanges before the initiation of the CANIGO project. This paper is an attempt to fill this gap.

One of the key problems in estimating any kind of transports through the Strait of Gibraltar is the time variability of the water flow itself. The fluctuations around the mean value can be roughly classified into three categories: tidal, sub-inertial (mainly meteorologically forced fluctuations) and seasonal (Lacombe and Richez, 1982; Candela et al., 1989, 1990; García-Lafuente et al., 2000, 2002). Only tidal fluctuations have been considered in this work. Because of the strong stratification and the steep topography existing in the strait, the tide shows a baroclinic character; that is, the amplitude and phase of both tidal current and tidal oscillation of isopicnals are strongly depth-dependent. This can be explained as the superposition of a barotropic tide with a perturbation generated in Camarinal Sill that radiates east- and westward (Candela et al., 1990). In the eastern section, tidal currents at the lower layer are strong enough to reverse the "mean" flows, so that during almost half tidal cycle the water in the lower layer flows back into the Mediterranean Sea. Tidal velocities in the upper layer at this section decrease by a factor of three compared to those in the lower layer, and are generally too weak to produce current reversals (García-Lafuente et al., 2000). Contrary to what happens at Camarinal Sill section, in the western entrance of the Strait (Bryden et al., 1994), the calculations at the eastern section show that the contribution of tidally rectified transports to the total transport is negligible ($<5\%$, García-Lafuente et al., 2000). This allows us to remove tidal variability and then to use the zero-mean-current surface as the separation between mean inflow and outflow in order to estimate transports.

The objective of the present work is to estimate the plankton biomass transport through the eastern section of the Strait of Gibraltar from direct measurements of current velocity and plankton biomass concentration. Fluxes are also estimated for different functional and taxonomic groups of the microbial community. The influence of short-term time variability (for a one-day period), on the fluxes estimates is assessed. Finally, a comparison with different estimates assuming less spatial resolution in both velocities and biomass is performed.

2. Material and methods

2.1. Current velocity measurements

From October 1995 to April 1998, three mooring lines with Aanderaa current meters were deployed at the eastern section of the Strait of Gibraltar in the context of the interdisciplinary European project CANIGO (Fig. 1). The moorings were situated at the northern (Nm site in Fig. 1c, five current meters), central (Cm, seven units) and southern (Sm six units) locations of the section. The sampling interval was 1 h. Fig. 2 describes the precise time sequence of measurements taken at each mooring, and Fig. 3 shows the three mean velocity profiles, along with the standard deviation associated with tidal currents.

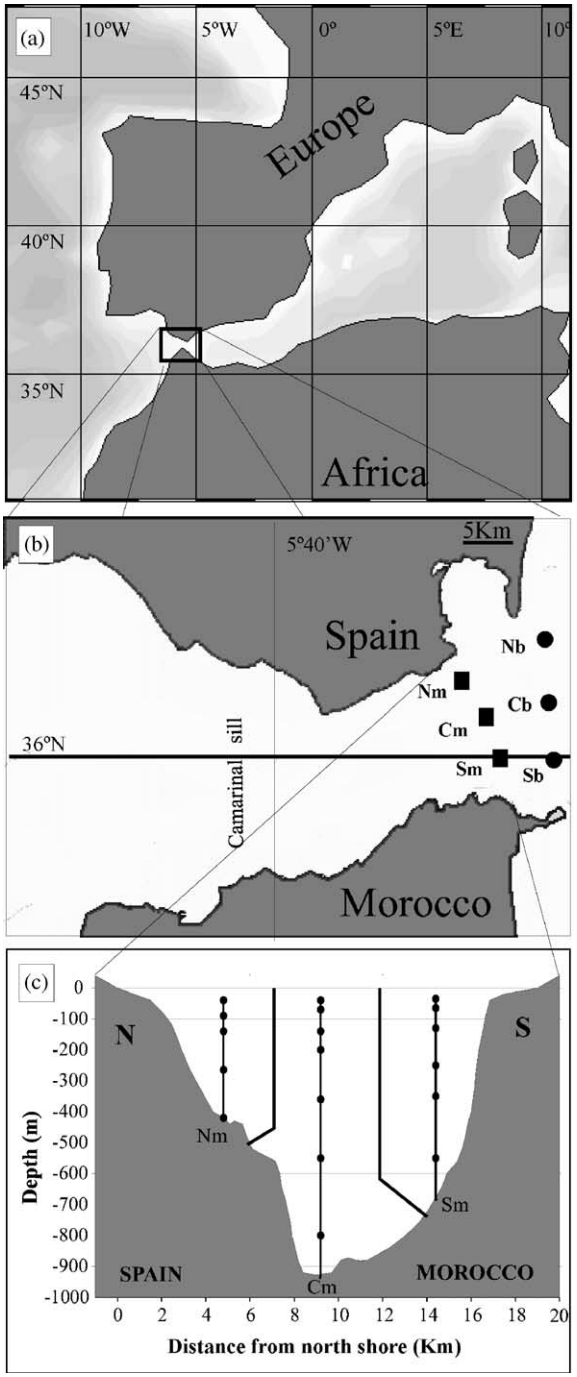

Fig. 1. (a) Sampling site. (b) Location of the northern (Nm), central (Cm) and southern (Sm) mooring lines and biological (Nb, Cb, Sb) sampling stations. (c) Vertical cross section of the mooring array (black points represent current-meter locations), and the three subsections for which transport has been estimated.

2.2. CTD profiles and biological sampling

In September 1997 a cruise on board *R.V. Thalassa* was carried out in the Strait of Gibraltar, within CANIGO. Three stations were studied at consecutive days (7–9 September 1997) in a section 8 km east of the current-meter moorings (Fig. 1b) . Six, ten, and five CTD (Neil Brown Mark III)-rosette casts were carried out at the northern (Nb), central (Cb) and southern (Sb) sampling stations (these are referred as stations number 6, 7 and 8, respectively, in other contributions of this issue).

Biological sampling at Nb and Sb were carried out at approximately 9:30 GMT. At station Cb, the sampling extended during a complete 24-h period with a time interval of approximately 4 h. Nine to eleven sampling depths were selected from the salinity and temperature vertical profiles provided by the CTD of the rosette, in order to properly sample the inflowing, outflowing layers, as well as the thermocline and the halocline. Due to the intrinsic vertical heterogeneity of biological variables, higher sampling resolution was used in the upper 100 m. Subsamples from each bottle were taken as follows: (i) 20 ml were preserved with glutaraldehyde (2% f.c.) and stored in cold and dark for less than two weeks to carry out the analysis of abundance and biomass of heterotrophic bacteria and flagellates; (ii) 4 ml were preserved with glutaraldehyde (1% f.c.) and stored in liquid nitrogen for flow cytometric analysis of autotrophic pico- and nanoplankton (0.2–20 μm ESD); (iii) 3000–3500 ml were filtered through 5 μm pore size mesh and the retained material preserved with hexamin-Na formaline for the analysis of microplankton (> 20 μm).

2.2.1. Laboratory analysis

Heterotrophic bacteria (HB) and flagellate abundance were determined by epifluorescence microscopy on samples stained with DAPI (Porter and Feig, 1980). Samples of 10 ml were stained and concentrated on 0.2 μm Nuclepore black filters and examined with a Leitz Dialux microscope equipped with a 2-∂ Ploemopack epifluorescence system. Bacteria were counted on 20 random, 2500 μm^2 fields. Heterotrophic (HNF) and autotrophic (ANF) nanoflagellates were dis-

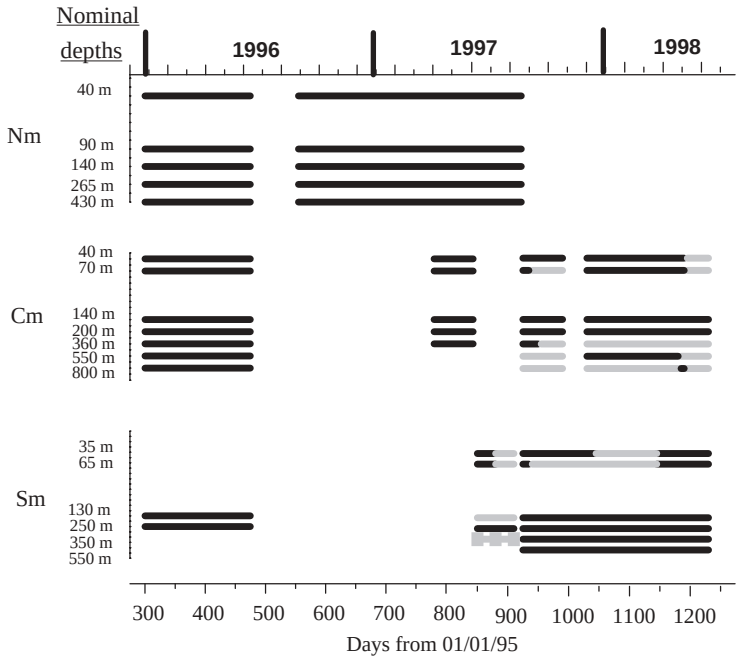

Fig. 2. Time schedule of current measurement. The nominal depths of the current meters are shown on the left axis. Periods of correct recording are represented by black lines. Periods of bad recording are represented by gray lines.

tinguished by switching from an UV (340–380 nm) to a blue (> 390 nm) filter, which reveals chlorophyll *a* fluorescence (Sherr et al., 1993). To estimate HNF abundance, at least 50 cells were counted in each sample. Bacteria and HNF size was measured on 11 representative samples. Cell biometry was carried out with a digital image analysis system composed of a photometrics digital video camera CCD sensys with a resolution of 1317×1035 pixels, and a Leica DMBL microscope. The calibration at $1000\times$ was 17.2 pixel μm^{-1}. Images were stored in TIF format and processed with the Image-Pro software. The resulting mean size distribution for each group was applied to produce biovolume estimates on the rest of the samples. Photoautotrophic plankton <20 μm were analysed with a Becton Dickinson FACScan flow cytometer, with an excitation laser of wavelength $\lambda = 488$ nm. The fluorescence signal >650 nm was ascribed to chlorophyll *a*, and fluorescence between 563 and 607 nm to phycoerythrin. These two fluorescence signals, together with forward- and side-light scatter, allow the identification and abundance estimate of *Synechococcus*, *Prochlorococcus* and eukaryotic pico- and nanoplankton (Fig. 4). Two different instrument settings were necessary to cover the high variability of natural communities (Table 1). The forward scatter signal was converted into biovolume by the equation

$$\mathrm{Bv} = 10^{-1.78+0.0055\mathrm{FSC}_{(E00)}} \quad (1)$$

(Jiménez Gómez, 1995), where Bv is biovolume (μm^3) and $\mathrm{FSC}_{(E00)}$ the channel of forward scatter (amplification E00). Microplankton were analysed following the method of Lund et al. (1958). At least 400 cells were counted and measured at $100\times$ and $250\times$ on a Leitz Fluovert inverted microscope connected to a CCD video camera (Kappa CF15/2) with a VIDS V (analytical measuring system) Image Analyser. Cell volume was estimated as the revolution volume according to an ellipsoidal or cylindrical shape. The respective cell volumes were converted into carbon by the formulae summarised in Table 2.

The sum of bacteria and HNF biomass in a size range of 0.2–10 μm will be referred as heterotrophic biomass, and the sum of the biomass of

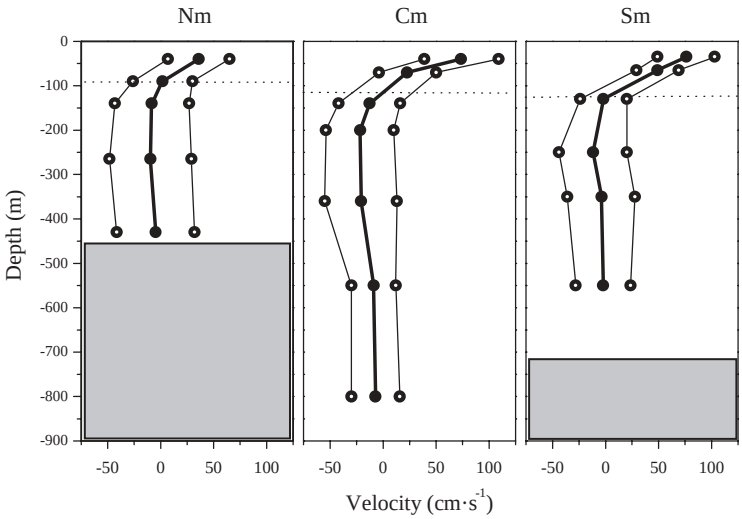

Fig. 3. Vertical profiles of the mean velocities (black circles) along with the standard deviation (open circles) associated with tidal currents. Dotted lines indicate the mean depth of zero velocity at each mooring. Gray boxes represent the seafloor.

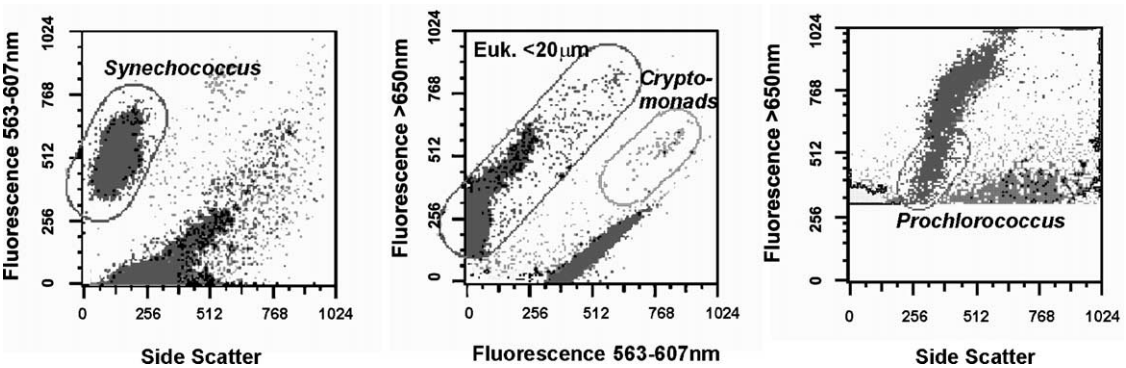

Fig. 4. Cytograms and attractors used to identify phototrophic prokaryota (*Synechococcus* and *Prochlorococcus*) and phototrophic eukaryotic pico- and nanoplankton. See text (methods) for details.

Table 1
Instrument settings applied to the FACScan (Becton Dickinson) Flow Cytometer. Setting (I) was used to analyse *Synechococcus*, eukaryotic picoplankton and eukaryotic nanoplankton, and setting (II) to analyse *Prochlorococcus* abundance

	Setting I	Setting II
Forward scattering	E00	E01
Side scattering	271	402
Fluorescence (> 650 nm)	300	651
Fluorescence (563–607 nm)	450	555

Prochlorococcus, *Synechococcus* and eukaryotic phytoplankton as autotrophic biomass.

3. Results

3.1. Distribution of biological groups

Fig. 5 represents the abundance vertical profiles of the biological groups considered in this study. The highest abundance and variability of both

Table 2
Conversion formulae used to estimate planktonic biomass

Biological Group	Formulae	Reference
HB	Bm = 0.38Bv	Lee and Fuhrmann (1987)
HNF	Bm = 0.22Bv	Borsheim and Bratbak (1987)
Synechococcus	Bm = 0.47Bv	Verity et al. (1992)
Eukariotic phytoplankton	Bm = $0.433(Bv)^{0.863}$	Verity et al. (1992)
Prochlorococcus	Bm = 0.053 cell	Morel et al. (1993)

Bm is biomass (pg C), Bv is biovolume (μm^3).

photoautotrophic and heterotrophic components of the planktonic community were found in the upper 100 m. Heterotrophic bacteria and flagellates, *Synechococcus* and microphytoplankton were most abundant at the northern station. *Prochlorococcus* and eukaryotic nano- and picoplankton, in contrast, showed their highest abundance at the southern station. Although numerically the photoautotrophic community was dominated by prokaryota (*Prochlorococcus* and *Synechococcus*) at all stations, in terms of biovolume (that is, taking into account the size distribution of populations) nanoplankton (2–20 μm cells) dominated biomass in the three stations (Fig. 6a), with similar absolute and relative biomass values in the uppermost surface layer. In contrast, large (> 20 μm) microplanktonic cells presented very low biomass values but increased their relative contribution slightly to the north. Total biomass concentration decreased with depth and from north to south (Fig. 6b).

3.2. Plankton biomass transport

For the estimate of biomass fluxes through the strait, time-averaged velocities were calculated for each current meter (Fig. 3). The respective biomass concentrations are obtained from the biological sampling at about 9:30 GMT at Nb and Sb stations and about 7:00 GMT at Cb station. We assume that the biomass concentration measured at one instant of time is representative of its time-averaged value or, in other words, it has a little deviation from its mean value. This assumption is tested in Section 3.3 where the variability of the estimates through a one-day period at the central subsection is assessed.

Transport estimates are carried out as follows: The cross-strait area is divided into three subsections (Fig. 1c), and each of them subdivided into 10-m bins. Then, vertical profiles of biomass concentration and velocity are linearly interpolated at the bin depths. Current-meter data in each mooring and rosette biomass at each station are thus considered representative for a whole subsection.The product of the interpolated profiles of concentration and velocity times the corresponding bin area is calculated at each bin. These values are then integrated from the surface to the depth of zero velocity, to obtain biomass import, and from the depth of zero velocity to the bottom, to obtain biomass export (Fig. 6b). Total biomass is finally estimated as the sum of the results of each of the three subsections. The entire process can be written as

$$I_{BT} = \sum_{i=1}^{3} \int_{z_{u=0}}^{\text{surface}} u_i(z) c_i(z) L_i(z)\, dz, \tag{2}$$

$$O_{BT} = \sum_{i=1}^{3} \int_{\text{bottom}}^{z_{u=0}} u_i(z) c_i(z) L_i(z)\, dz, \tag{3}$$

where I_{BT} and O_{BT} are inflowing and outflowing biomass transport respectively, u_i is the interpolated along strait velocity at bin i, c_i the biomass concentration, and L_i the bin width. Inflowing transport into the Mediterranean Sea is positive, while outflowing transport towards the Atlantic is negative. These calculations would be referred to a six boxes model, since the section has been divided into three boxes for the inflow and another three boxes for the outflow.

Imported and exported biomass estimates are 5570 and −1140 tonnes C day^{-1} respectively, that is, import is almost five times greater than export estimate. Table 3 shows the biomass flux estimate in each box. Both import and export show a maximum absolute value in the central boxes. However, each of the upper boxes accounts for a similar percentage of the total biomass import, while the lower central box alone contributes 70% to the total biomass export. Despite the fact that

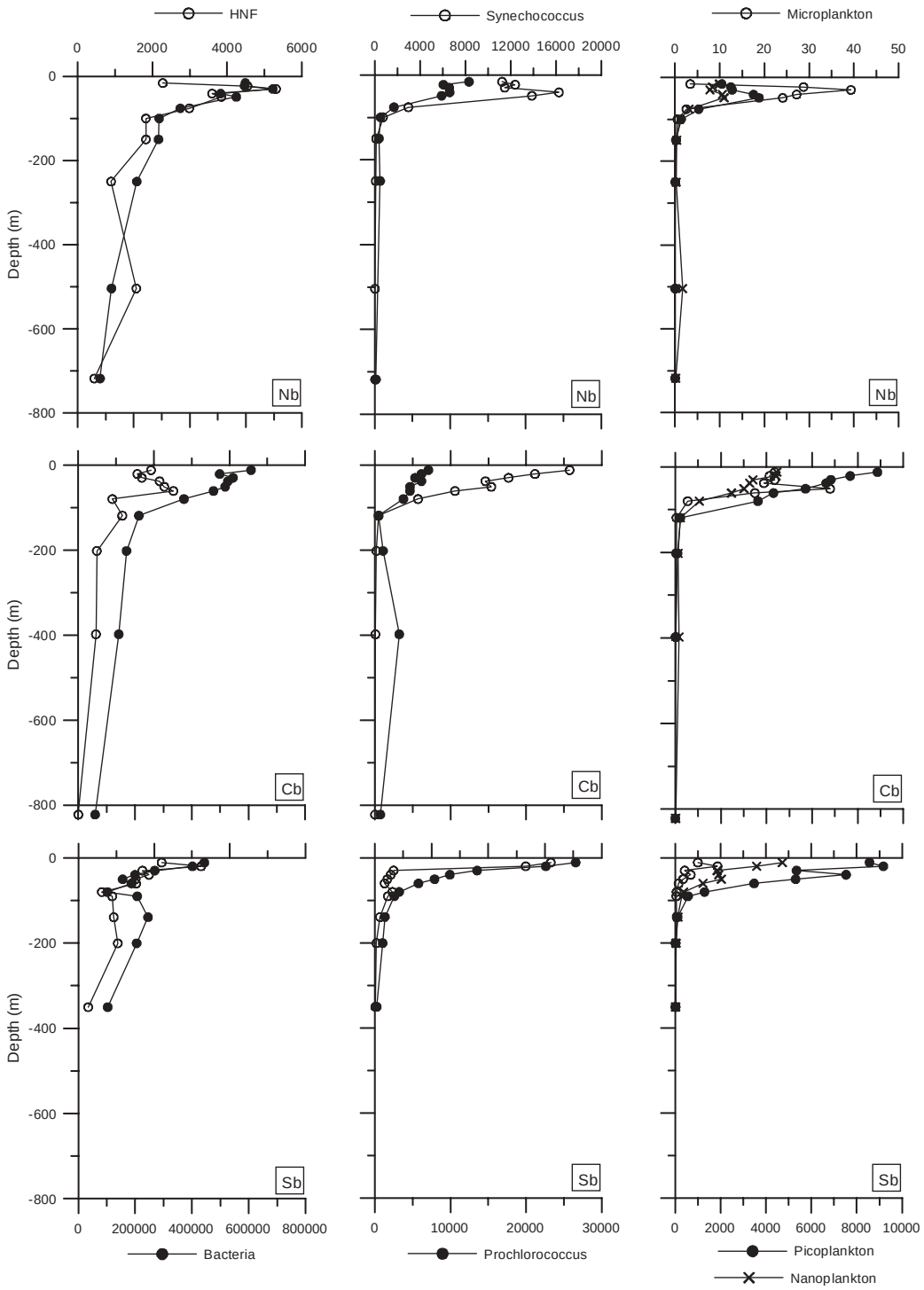

Fig. 5. Abundance (cells ml^{-1}) vertical profiles at biological stations: heterotrophic bacteria and heterotrophic nanoflagellates (first column), phototrophic prokaryotes *Prochlorococcus* and *Synechococcus* (second column), and phototrophic eukaryotes (pico-, nano- and microplankton, third column).

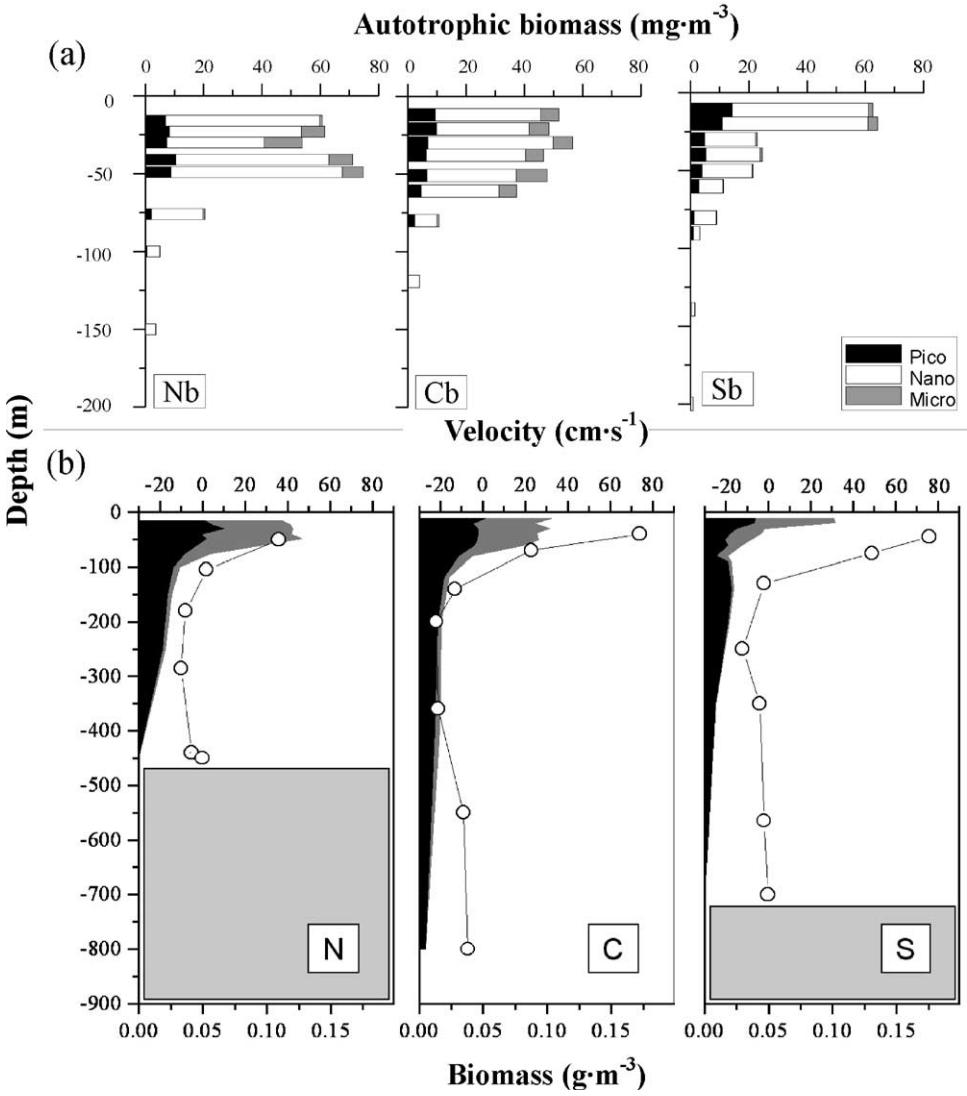

Fig. 6. (a) Profiles of phototrophic picoplankton, nanoplankton and microplankton at Nb, Cb, and Sb. (b) Vertical biomass profile (filled area) subdivided into heterotrophic (black area) and Photoautotrophic (gray area) organisms. The solid lines with open symbols are the mean velocity profiles at Nm, Cm and Sm. Gray boxes represent the seafloor.

the biomass concentration in the upper layer of Nb is higher than in Cb and Sb (Fig. 6), the contribution of the northern upper box to total biomass import is the lowest one, as a consequence of the low inflowing velocities found in Nm. On the contrary, high velocity at Sm compensates the low biomass concentration to give a relative important biomass import through the southern subsection.

Fractional biomass fluxes also have been estimated for all identified planktonic groups (Table 4). Autotrophic and heterotrophic organisms have similar contributions to the import ($\sim$56% and 44%, respectively). Exported biomass, in contrast, is dominated by heterotrophic organisms ($\sim$89%). Phototrophic nanoplankton is the main contributor to the autotrophic biomass exchange. In spite of their relative high abundance, autotrophic

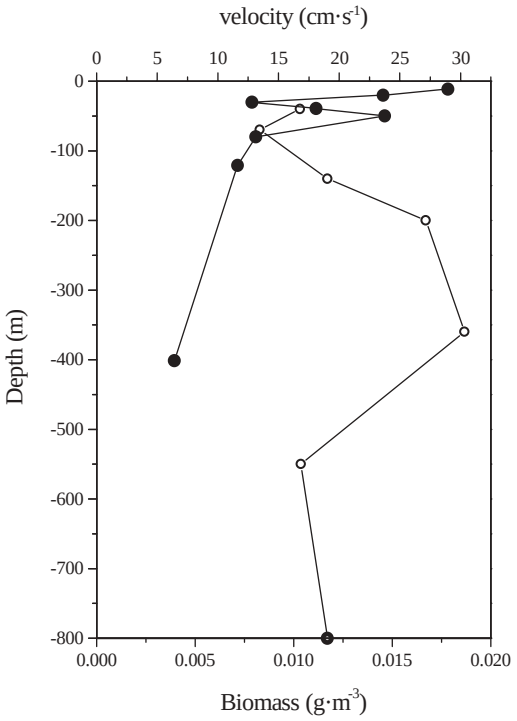

Fig. 7. Black circles: vertical profile of the standard deviation of biomass concentration at Cb. Open circles: vertical profile of the standard deviation of tidal currents at Cm.

Table 3
Biomass transports estimates in each box of the six-boxes, HR model

	N	C	S	Total
Import (Ton C day^{-1})	1380	2280	1910	5570
Import (%)	25	41	34	100
Export (Ton C day^{-1})	−180	−830	−130	−1140
Export (%)	16	73	11	100

Last column shows the total biomass transports estimates through the section.

prokaryotes (*Prochlorococcus* and *Synechococcus*) contribute only in around 5% to biomass import and in less than 1% to biomass export.

3.3. Time variability

Biomass transports are sensitive to the time variability of both flow and biomass concentration. Current data have been measured for a long period, so we can expect that the given mean values have little error. But we cannot say the same for the biomass concentration, as only a single measurement for each depth was available. To address this problem, station Cb was sampled during almost two complete semidiurnal cycles, allowing for an estimate of the variability during a one-day period (Fig. 7). These observations can be used to investigate the influence of the biomass variability on the estimated fluxes at the central subsection. Stations Nb and Sb were not sampled in the same way, and thus time variability cannot be assessed at the corresponding subsections.

The relative differences between the biological transports estimated in Section 3.2 from a single observation at the central subsection and the mean values obtained from the 24-h cycles, $(I_{BT})_0$ and $(O_{BT})_0$, are 1% and 13%, respectively. The inflowing transport estimate remains almost the same, while the outflowing transport estimate from a single measurement provides an underestimate of the mean value.

It is possible to derive a more robust estimate of the transport errors. Lets denote the error in velocity u_i and biomass concentration c at a given point as Δu and Δc, respectively. Assuming that the relative error of u is small in relation to the relative error of c, the absolute error of their product can be written as

$$\Delta(u \cdot c) = u \cdot \Delta c + \Delta u \cdot c \simeq u \cdot \Delta c. \quad (4)$$

Thus, integration of Eq. (4) from the interface to the surface and from the bottom to the interface gives the estimated errors for inflowing and outflowing transports:

$$\Delta(I_{BT}) \simeq \sum_{i=1}^{3} \int_{z_{u=0}}^{\text{surface}} u_i(z)\Delta c_i(z)L_i(z)\,dz, \quad (5)$$

$$\Delta(O_{BT}) \simeq \sum_{i=1}^{3} \int_{\text{bottom}}^{z_{u=0}} u_i(z)\Delta c_i(z)L_i(z)\,dz, \quad (6)$$

where $\Delta c_i(z)$ stands for the interpolated standard deviation of biomass concentration at bin i. The estimated errors calculated on this way are 300 tonnes C day^{-1} (around 13% of the mean value) for the inflowing, and 200 tonnes C day^{-1}

Table 4
Relative contribution (%) of each identified group to the biomass transport, at each subsection, and to the total biomass transport through the section

	North		Centre		South		Total	
	In	Out	In	Out	In	Out	In	Out
HB	39	77	37	73	35	84	37	75
HNF	8	12	6	15	8	11	7	14
Prochlorococcus	1	<1	<1	1	2	<1	1	<1
Synechococcus	4	<1	5	<1	4	<1	5	<1
Eukaryotic picoplankton	1	<1	2	<1	6	0	3	<1
Eukaryotic nanoplankton	42	10	42	9	42	4	42	9
Eukaryotic microplankton	5	<1	7	1	2	<1	5	<1

(around a 24%) for the outflowing transport. These are higher values than the estimated error for the single measurement. Thus, it can be concluded that the different effects acting during a 24-h period (biological distribution, tidal currents) may change the inflowing biological transport by approximately 10–15%, and the outflowing biological transport by 25%, relative to their mean values. This result is valid only for the central subsection, and its application to the whole section should be made with caution. In any event, our initial assumption that biomass transport can be calculated with reasonable accuracy (approximately 10–15%) using a single profile per station is confirmed, at least for the inflowing transport at the central subsection, giving a relative support to the total biomass transport estimated for the entire eastern section.

4. Discussion

4.1. Biological variability

There are several factors that may affect the spatial distribution and size-structure of the planktonic community, as the presence of different water masses in the region, the variability of the vertical position and intensity of the transition between them (the so-called Atlantic–Mediterranean Interface, AMI, Section 4.2), the gradients of temperature (seasonal thermocline) and of horizontal velocity. For example, the northwestward shoaling of the AMI (Echevarría et al., 2002), approaching to the thermocline (Gómez et al., 2000), may trigger processes that facilitate the fertilisation of the upper layer in the manner proposed by Rodríguez et al. (1998) for the Alborán Sea.

It seems that these processes produce a relevant effect on the size structure of the phytoplanktonic community. According to the relation between vertical dynamics, the trophic status of the surface layer, and the position of the AMI proposed by Rodríguez et al. (1998), a shallow AMI should be indicative of a phytoplankton community whose biomass is dominated by large cells (microplankton). Increasing chlorophyll concentrations towards Nb in June and September 1997 are described by Echevarría et al. (2002). However, the shoaling of the AMI towards the north in the studied section (Fig. 8) does not parallel the biomass dominance of microplankton, but shows only a slight increase of its relative contribution to a community where nanoplankton represents 62–98% of autotrophic carbon biomass throughout the Strait. Chisholm (1992) suggested that microplankton dominance is usually found at chlorophyll concentration values higher than 2 $\mu g\, l^{-1}$. In station Nb, the chlorophyll concentration is around 2.5 $\mu g\, l^{-1}$ at the level of the deep maximum (Gómez et al., 2000), whereas the chlorophyll concentration found by Rodríguez et al. (1998) in the northwestern Alborán Sea was 7–8 $\mu g\, l^{-1}$. This could explain the relatively low contribution of microplankton to total biomass even in station Nb, where a shallow AMI would provide favourable conditions for the

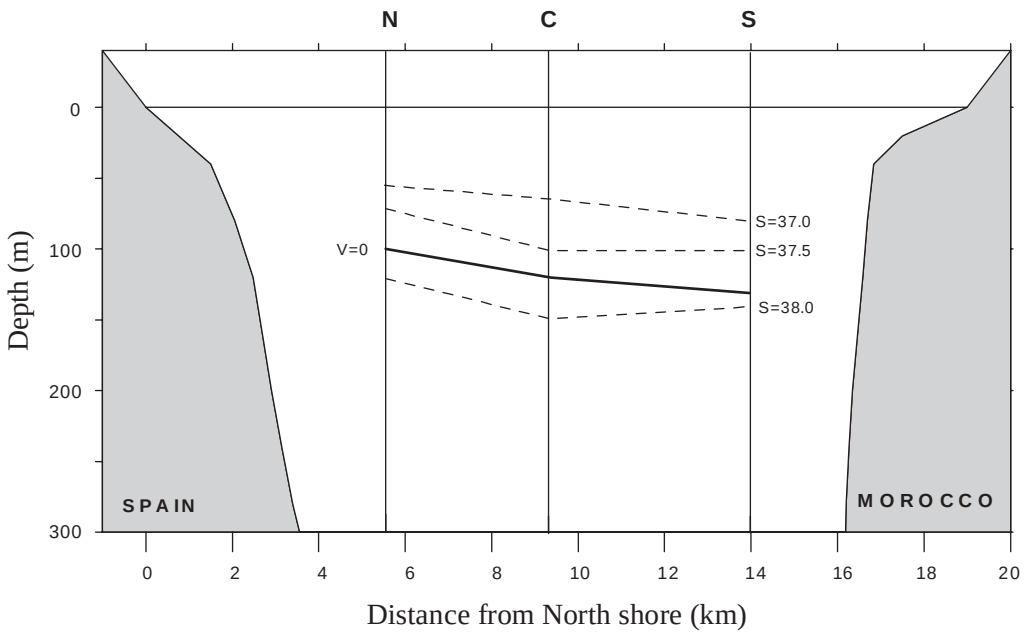

Fig. 8. Cross-section of the eastern section with sketches of the mean zero-velocity depth (solid line). As orientation, the $S =$ 37.0, 37.5 and 38.0 isohalines obtained from CTD casts at the biological stations are also sketched.

growth and biomass accumulation of microplankton. Heterotrophic biomass accounts for 24–96% of planktonic biomass at the eastern section and highest absolute values coincide with the autotrophic biomass maximum (Fig. 6b).

4.2. The position of the interface and its influence on fluxes estimates

Estimating the fluxes between the Atlantic and the Mediterranean necessitates defining the boundary between the two opposite currents and its changing position. In terms of water properties, the AMI is the layer in which salinity changes from "Atlantic" to "Mediterranean" values, that is, from approximately $S \sim 36.5$–38.4 (Lacombe and Richez, 1982). In the present work, these later values will be used to operationally define the AMI. It presents a finite thickness, and rigorously cannot be defined by a single depth but rather by a range of them. Gascard and Richez (1985) define the AMI as the layer between 37.0 and 37.5, and as such it has been analysed by Rodríguez et al. (1998) in the Alborán Sea. However, other authors have identified the depth of the AMI with that of a single isohaline. When following this procedure, care must be taken to justify the specific salinity value. For example, Bryden et al. (1994) selected 37.0 and found a good correlation between this isohaline depth and the instantaneous level of no motion at the sill region of the Strait.

In our calculations, we have used the zero-mean-current depth derived from the moored current meters as the separation between inflow and outflow: ~ 100 m in Nm, ~ 120 m in Cm, and ~ 130 m in Sm (Fig. 8). This depth locally coincides with the mean depth of the 37.9 isohaline, as shown by García-Lafuente et al. (2000). This salinity is higher than those used by Gascard and Richez (1985) or Bryden et al. (1994), and is located at the lower depth range of the AMI. Consequently, interfacial waters at the eastern part of the Strait mainly flow into the Mediterranean, as suggested by Bray et al. (1995).

It has been customary to assume a near-zero horizontal velocity linked to the 37.0–37.5 iso-

halines (Coste et al., 1988; Gómez et al., 2000). However, it would be more appropriate to assume salinity values closer to $S = 38.0$ for the depth of mean zero velocity at the Mediterranean side of the Strait, if no in situ current data are available.

4.3. Other approaches to biomass transport estimates: influence of spatial variability

It is important to address the influence of spatial heterogeneity of both velocity and biomass concentration in transport estimates. Here, a comparison of the chosen approach with two other different approaches is made: In the first one, the vertical variation of velocity and biomass concentration is ignored. In the second one both the vertical and horizontal variations are ignored.

4.3.1. Vertical variation ignored

The estimated biomass transports can be calculated by multiplying the depth-averaged biomass concentration by the water transport through each box. These water transports are obtained using the velocity profiles of Fig. 3 and the geometry of Fig. 1c, that is, using Eqs. (2) and (3) with $c_i = 1$. The estimates are 3880 and -1240 tonnes C day^{-1} for the import and export, respectively. This approximation gives 30% less biomass import and 9% more biomass export through the whole eastern section than the Higher Resolution estimate (HR hereafter), which takes into account the vertical variability. The respective values for each box (Table 5) reveal that the import underestimation is high, while export estimates are less sensitive because of the relatively homogeneous profiles of both variables in the lower layer. Thus, the vertical variability of both biomass and velocity affects mainly the estimate of the imported biomass, and the underestimate is higher in the central and southern upper boxes.

4.3.2. Vertical and horizontal variation ignored

It is assumed that only the values of total inflow and outflow are available. The biomass import (export) estimate would be obtained as the product of a mean inflow (outflow) times a mean biomass concentration in the upper (lower) layer. The value of 0.8 Sv, which is the sum of the three partial flows obtained above, is used in this case. The biomass concentration in each layer is calculated as the mean value of the three depth-averaged biomass concentrations in Nb, Cb and Sb. The results are 4250 and -1070 tonnes C day^{-1} for the import and export, respectively. This more simple bulk approach still underestimates the HR computation (24% for the import, 6% for the export), but it leads to more realistic values than in the first test. The reason is that biomass concentration and velocity profiles increase towards the surface, but they show an opposite distribution across the Strait.

These tests indicate that any transport estimate of patchy distributed variables, like biomass concentration, through the Strait of Gibraltar based on bulk measurements or with low spatial resolution must be considered cautiously.

5. Limitations

The values proposed in the present work are based on water-flux estimates and biomass concentrations measured with reasonable spatial and temporal resolution. However, there are some aspects and strategies of the experimental design that also must be considered.

First, the sections of biological casts and current measurements lay ~ 8 km apart in the along-Strait direction, shedding some doubts about the spatial coherence of the vertical profiles. The AMI rises from west to east, and the mean interface slope at the eastern section of the Strait is of the order of 1 m/km (Bray et al., 1995, Fig. 5a). The distance between both sections is thus short enough to prevent the profiles from changing significantly.

Another question of concern is the lack of near-surface current measurements. This is partially due to the difficulty of deploying instruments close to the surface in a region of heavy traffic ship and fishing activity like the Strait of Gibraltar. The mooring lines were designed to place the uppermost current meter at depths of 30–40 m. Therefore, near-surface currents have been extrapolated.

The influence of daily variability on the exchanged biomass has been examined, but other intermediate frequencies variability (as the influ-

Table 5
Biomass transport estimates for each box in the six-boxes approach, calculated by multiplying the depth-mean biomass of each box with the respective mean water transport

	N	C	S
Import estimate	960 (25%)	1720 (44%)	1180 (30%)
Difference with HR estimate	−420 (−30%)	−560 (−24%)	−730 (−38%)
Export estimate	−250 (20%)	−870 (70%)	−130 (10%)
Difference with HR estimate	70 (40%)	40 (5%)	0 (0%)

It is also shown the difference with the HR estimate in Table 3. Units are ton day^{-1}.

ence of meteorologically forced current fluctuations and the fortnightly cycle) have not. The reason is that the short time allowed for the biological sampling did not allow it.

The seasonal variation of the fluxes also must be considered. García-Lafuente et al. (2002) have estimated a seasonal cycle for the water inflow of $(10\pm5)\%$ its mean value, with the maximum in middle August. Thus, it could be possible to correct the inflowing biological transport given above by a similar amount. However, biomass concentration also may exhibit important seasonal fluctuations, specially in the upper part of the water column. Therefore, the seasonal cycle, although statistically significative, still has a great uncertainty, and there is no estimate of seasonal variation in primary production. The obtained values are assumed to be representative for late summer conditions, and it is recognised that more field sampling (specially of biomass concentrations), over longer periods, is needed in the future.

In spite of the temporal variability of biomass concentrations, the described spatial distribution pattern of autotrophic biomass in the cross-Strait section was also found in terms of chlorophyll *a* concentration in June 1997 (Echevarría et al., 2002) and seems to be typical for the study area.

Finally, in evaluating basin-scale's balances between the Mediterranean and the Atlantic, it should be taken into account that an unknown fraction of the biomass fluxes measured at the studied section may be recirculated and/or generated within the Strait (see Echevarría et al., 2002, for an estimate of the latter). In particular, Gómez et al. (2000) and Echevarría et al. (2002) suggest that the fertilisation of the upper Atlantic layer due to mixing at Camarinal Sill (see Fig. 1) may increase in-situ primary production and the biomass content of the layer crossing the section towards the Mediterranean. The measurement of primary production in the Strait therefore appears necessary to test this hypothesis and to achieve a biomass balance between both basins.

6. Conclusions

Biomass transports have been estimated at the eastern section of the Strait of Gibraltar. The biomass import and export are estimated to be approximately 5600 and −1100 tonnes C day^{-1}, respectively. Photoautotrophic organisms account for approximately 50% of imported biomass, while exported biomass is dominated by heterotrophic organisms ($\sim$90%). Both, the planktonic biomass balance and functional composition support the suggestion of Coste et al. (1988) that the Mediterranean acts as a mineralization area.

The influence of one-day time variability in the calculations have been estimated at the central location. The variation is around 15% for inflowing biomass transport and 25% for outflowing biomass transport. The spatial resolution of the estimates also has been assessed: estimates with lower spatial resolution tend to underestimate the biomass import, while biomass export is rather insensitive to the spatial resolution of the calculations.

Finally, the recognised limitations of the available data make necessary more extensive field work in the future to validate the values estimated in the present work.

Acknowledgements

This work was supported by the European Commission through CANIGO project (MAS3-CT96-0060). We are also grateful to the Captain and crew of the *R/V Thalassa* from IEO/IFREMER, and to the Captains and crews of the R.V.'s *Tofiño*, from Instituto Hidrográfico de la Marina, Cádiz, Spain; *Odón de Buen* from IEO; and *Poseidon* from IFM Kiel, for their help in the deployment and recovery of the mooring lines.

References

Armi, L., Farmer, D.M., 1985. The internal hydraulics of the Strait of Gibraltar and associated sills and narrows. Oceanologica Acta 8, 37–46.

Armi, L., Farmer, D.M., 1988. The flow of Mediterranean water through the Strait of Gibraltar. Progress in Oceanography 21, 1–105.

Borsheim, K.Y., Bratbak, G., 1987. Cell volume to cell carbon conversion factors for a bacteriovorous. Monas sp. enriched from seawater. Marine Ecology Progress Series 36, 171–175.

Bray, N.A., Ochoa, J., Kinder, T.H., 1995. The role of the interface in the exchange through the Strait of Gibraltar. Journal of Geophysical Research 100, 10 755–10 776.

Bryden, H.L., Kinder, T.H., 1991. Steady two-layer exchange through the Strait of Gibraltar. Deep-Sea Research I 38 (1), S445–S463.

Bryden, H.L., Candela, J., Kinder, T.H., 1994. Exchange through the Strait of Gibraltar. Progress in Oceanography 33, 201–248.

Candela, J., Winant, C.D., Bryden, H.L., 1989. Meteorologically forced subinertial flows through the Strait of Gibraltar. Journal of Geophysical Research 94, 12 667–12674.

Candela, J., Winant, C.D., Ruiz, A., 1990. Tides in the Strait of Gibraltar. Journal of Geophysical Research 95, 7313–7335.

Chisholm, S.W., 1992. Phytoplankton size. In: Falkowski, P.G., Woodhead, A.D. (Eds.), Primary Productivity and Biogeochemical Cycles in the Sea. Plenum Press, New York, pp. 213–237.

Coste, B., Le Corret, P., Minas, H.J., 1988. Re-evaluation of nutrient exchanges in the Strait of Gibraltar. Deep-Sea Research 35 (5), 767–775.

Echevarría, F., García-Lafuente, J.G., Bruno, M., Gorsky, G., Goutx, M., González, N., García, C.M., Gómez, F., Vargas, J.M., Pichesal, M., Striby, L., Varela, M., Alonso, J.J., Revel, A., Cózar, A., Prieto, L., Sarhan, T., Plaza, F., Jiménez-Gómez, F., 2002. Physical-biological coupling in the Strait of Gibralter. Deep-Sea Research II 49 (19), 4115–4130.

García-Lafuente, J., Vargas, J.M., Plaza, F., Sarhan, T., Candela, J., Bascheck, B., 2000. Tide at the eastern section of the Strait of Gibraltar. Journal of Geophysical Research 104 (C2), 3109–3119.

García-Lafuente, J., Delgado, J., Vargas, J.M., Vargas, M., Plaza, M., Sarhan, T., 2002. Low-frequency variability of the exchanged flows through the Strait of Gibraltar during CANIGO. Deep-Sea Research II 49 (19), 4051–4067.

Gascard, J.C., Richez, C., 1985. Water masses and circulation in the western Alboran Sea and in the Strait of Gibraltar. Progress in Oceanography 15, 157–216.

Gómez, F., Echevarría, F., García, C.M., Prieto, L., Ruiz, J., Reul, A., Jiménez-Gómez, F., Varela, M., 2000. Microplankton distribution in the Strait of Gibraltar: coupling between organisms and hydrodynamic structures. Journal of Plankton Research 22 (4), 603–617.

Jiménez Gómez, F. 1995. Estructuras de tamaños y dinámica del ultraplankton en el ecosistema pelágico. Ph.D. Thesis, Univ., Málaga, Spain, unpublished.

Lacombe, H., Richez, C., 1982. The regime of the Strait of Gibraltar. In: Nihoul, J.C.J. (Ed.), Hydrodynamics of Semi-enclosed Seas. Elsevier Oceanography Series 34. New York, pp. 13–73.

Lee, S., Fuhrmann, J.A., 1987. Relationships between biovolume and biomass of naturally derived marine bacterioplankton. Applied Environmental Microbiology 53, 1298–1303.

Lund, J.W.G., Kipling, C., Le Cren, E.D., 1958. The inverted microscope method of estimating algal numbers and the statistical basis of estimates by counting. Hydrobiologia 11, 143–170.

Morel, A., Ahn, Y.-H., Partensky, F., Vaulot, D., Claustre, H., 1993. *Prochlorococcus and Synechococcus*: a comparative study of their optical properties in relation to their size and pigmentation. Journal of Marine Research 51, 617–649.

Porter, K.G., Feig, Y.S., 1980. The use of DAPI for identifying and counting aquatic microflora. Limnology and Oceanography 25 (5), 943–948.

Rodríguez, J., Blanco, J.M., Jiménez-Gómez, F., Echevarría, F., Gil, J., Rodríguez, V., Ruiz, J., Bautista, B., Guerrero, F., 1998. Patterns in the size structure of the phytoplankton community in the deep chlorophyll maximum of the Alboran Sea (southwestern Mediterranean). Deep-Sea Research I 45, 1577–1593.

Sherr, E.B., Caron, D.A., Sherr, B.F., 1993. Staining of heterotrophic protists for visualization via epifluorescence microscopy. In: Kemp, P.F., Sherr, B.F., Cole, J.J. (Eds.), Handbook of Methods in Aquatic Microbial Ecology. Lewis Publishers, London, pp. 213–227.

Verity, P., Robertson, C.Y., Tronzo, C.R., Andrews, M.G., Nelson, J.R., Sieracki, M.E., 1992. Relationships between cell volume and carbon and nitrogen content of marine photosynthetic nanoplankton. Limnology and Oceanography 37 (7), 1434–1446.